AGU PUBLICATIONS

JGR

Journal of Geophysical Research: Biogeosciences

RESEARCH ARTICLE
10.1002/2016JG003618

Key Points:
- High similarity in $\delta^{15}N$ is found between subsurface nitrate and particles regardless of size fractions in the euphotic zone
- Lateral transport of ^{15}N-depleted resuspended sediments contributes to a downward decreasing trend of $\delta^{15}N$ in sinking particles
- The significant change of $\delta^{15}N$ in sinking particles in the water column makes the South China Sea different from most other marginal seas

Correspondence to:
S.-J. Kao,
sjkao@xmu.edu.cn

Citation:
Yang, J.-Y. T., S.-J. Kao, M. Dai, X. Yan, and H.-L. Lin (2017), Examining N cycling in the northern South China Sea from N isotopic signals in nitrate and particulate phases, *J. Geophys. Res. Biogeosci.*, *122*, doi:10.1002/2016JG003618.

Received 19 OCT 2016
Accepted 25 JUL 2017
Accepted article online 14 AUG 2017

Examining N cycling in the northern South China Sea from N isotopic signals in nitrate and particulate phases

Jin-Yu Terence Yang[1,2], Shuh-Ji Kao[1], Minhan Dai[1], Xiuli Yan[1], and Hui-Ling Lin[3]

[1]State Key Laboratory of Marine Environmental Science, College of Ocean and Earth Sciences, Xiamen University, Xiamen, China, [2]Now at Division of Environmental Science and Engineering, Pohang University of Science and Technology, Pohang, South Korea, [3]Department of Oceanography, National Sun Yat-sen University, Kaohsiung, Taiwan

Abstract Nitrogen sources and dynamics, one of the key issues in marine biogeochemical cycles, remain poorly constrained in marginal seas. Here we examine the nitrogen cycle in the northern South China Sea (SCS) by combining data from previous reports with a new data set of N isotopic compositions ($\delta^{15}N$) of nitrate, zooplankton, and sinking particles. Average $\delta^{15}N$ in subsurface nitrate is 4.8 ± 0.3‰, similar to that of sinking particles ($\delta^{15}N_{sink}$ of 4.4‰) through the euphotic zone (EZ) collected by floating traps and to documented mean (4.6‰) for long-term mooring traps at 200 m. This along with oft-observed shallow nitracline (<100 m) suggests that subsurface nitrate is the primary source of new N to support export production. Moreover, $\delta^{15}N_{sink}$ at the bottom of the EZ resembles those of suspended particles (4.2 ± 1.0‰) and zooplankton (5.4 ± 1.0‰) inside the EZ. High similarity in $\delta^{15}N$ among various types of particles including zooplankton in different size fractions in the EZ implies rapid N turnover in the ecosystem. In deep waters at 2000–3000 m, however, additional particulate N fluxes are found due to lateral transport, which contain ^{15}N-depleted particles, resulting in a downward decreasing trend of $\delta^{15}N_{sink}$. Incorporation of lighter N by bacteria and selective export of picoplankton are proposed as alternative mechanisms contributing to low $\delta^{15}N_{sink}$ in the deep waters. The significant $\delta^{15}N_{sink}$ change in the deep water column makes the SCS different from most other marginal seas; thus, caution should be made when using sedimentary $\delta^{15}N$ to reconstruct paleonitrogen processes.

1. Introduction

Nitrogen isotopic composition ($\delta^{15}N$) of upwelled nitrate to the euphotic zone (EZ) could be imprinted on settling particulate organic matter (POM) and ultimately be buried in the sediments. For example, spatial patterns of sedimentary $\delta^{15}N$ in the polar and equatorial oceans have been proven to reflect surface ocean nitrate utilization [e.g., *Altabet and Francois*, 1994]. Furthermore, the $\delta^{15}N$ values of POM and sedimentary N in oligotrophic oceans are suggested to evidently signal new N from the subsurface waters and atmosphere [e.g., *Altabet et al*., 1991; *Gaye et al*., 2009; *Kao et al*., 2015]. In the continental margins or marginal seas, previous studies suggest that bulk N isotopic signatures of POM can be well preserved in sediments with minimal isotopic alteration during sinking and burial, primarily on account of relatively high sedimentation rates [e.g., *Robinson et al*., 2012, and references therein]. However, variable N sources and complexities of depositional environments in some large marginal seas such as the South China Sea (SCS) and the Mediterranean Sea may have challenging situations when evaluating N isotopic signals incorporated into particulate and sedimentary N [*Robinson et al*., 2012]. For example, a significant offset of bulk sedimentary $\delta^{15}N$ between two cores of nearby sites had been found on the northern slope of the SCS during the last glacial period, which was most likely caused by different origins of both organic and inorganic N at each site [*Kienast et al*., 2005].

The SCS, located in the tropical and subtropical regions of the western North Pacific, is one of the largest marginal seas in the world. It possesses a broad continental shelf (~40.5% of total area) and an oligotrophic deep basin (>5000 m). The biogeochemical cycles in the SCS basin are under the influence of the East Asia monsoon system and wind-induced mixing. Specifically, the primary production in the SCS shows a strong peak in winter and a weak peak in summer [*Liu et al*., 2002]. Seasonal variability in export production is generally insignificant based on observed and simulated results [*Cai et al*., 2015; *Liu et al*., 2002], although some studies show higher nitrate-based new production in winter [e.g., *Chen*, 2005].

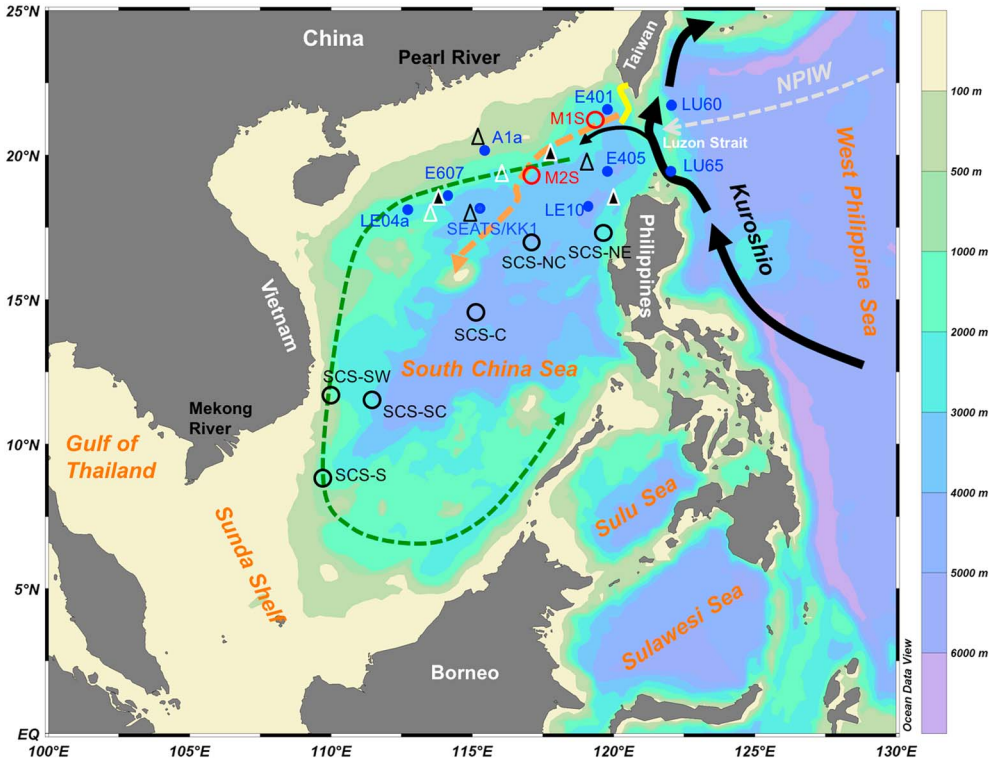

Figure 1. Locations of the M1S and M2S sites (red open dots) and KK1 for sinking particle, and of sampling sites for nitrate (blue solid dots) in the northern SCS and WPS. Sampling sites for zooplankton are shown as black (winter) and white (summer) open triangles (the same sites both for summer and winter are shown in filled ones, see Table 2). We also mark the deployment sites of sediment traps in the central and southern SCS from previous studies (Table 1). Current systems are also shown [*Liu et al*., 2016; *You et al*., 2005]: SCS deep water current (orange), surface current in winter (green), the Kuroshio Current (black), and the North Pacific Intermediate Water (NPIW, gray). The area of the Kaoping Canyon is marked as yellow. The color bar indicates water depth.

In contrast to commonly recognized river-dominated ocean margins, the SCS is recently proposed as an ocean-dominated margin [*Dai et al*., 2013] characterized by intensive interactions with the West Philippine Sea (WPS) via the Luzon Strait (LS), the unique channel for deep water exchange (Figure 1). Since the distribution of nutrient concentrations is quite different between the SCS and WPS, the nutrient budget in the SCS can thus be significantly influenced by interaction with the WPS. For example, the western boundary current, the Kuroshio, intrudes during winter and brings low nutrient, warm and saline water into the SCS surface [*Du et al*., 2013]. On the other hand, the SCS is thought to be a cul-de-sac of the subtropical North Pacific Intermediate Water (NPIW) [*You et al*., 2005], which may carry an isotopic signal from the Eastern Tropical North Pacific (ETNP). The SCS thus potentially archives the paleoinformation of the Asian monsoon, the intensity of the western boundary current, and the NPIW intrusion. Indeed, prior studies had suggested that bulk sedimentary $\delta^{15}N$ records from the SCS cannot be limited to the reconstruction of local/regional phenomena and may also have global implications [e.g., *Higginson et al*., 2003; *Kienast*, 2000]. However, ambiguities still exist regarding the N-cycling processes in the water column and the interpretation of paleorecords due to the lack of a comprehensive survey of N dynamics in the SCS.

To better define the $\delta^{15}N$ value of POM exported from the surface ocean and the isotopic record in sediment, nitrate $\delta^{15}N$ ($\delta^{15}N_{NO3}$) is crucial; however, there are to date only a few profiles of $\delta^{15}N_{NO3}$ reported in the upper water column of the SCS and adjacent regions [*Liu et al*., 1996; *Loick et al*., 2007; *Wong et al*., 2002]. Given the lack of basin-wide $\delta^{15}N_{NO3}$ data, it is not yet possible to well understand the isotopic endmembers of the major sources of new N and the sinking POM from the EZ, although some N isotope data of suspended POM in the EZ and sinking POM trapped in various depths had been reported in the SCS [*Gaye et al*., 2009; *Kao et al*., 2012; *Loick et al*., 2007].

Table 1. Sampling Information of All Data Sets of N Isotopes in Different N Components From the South China Sea (SCS) Basin and Adjacent Regions Used in This Study

Location (Site No.)	Time of Sampling	Sampling Depth	Data Source
	Nitrate		
Northern SCS (n = 7)	May 2011	0–4000 m	This study
WPS (n = 2)	May 2011	0–5000 m	This study
	Suspended Particle		
SEATS	2004–2007	0–200 m	*Kao et al.* [2012]
Central SCS (n = 2)	September 1981	0–4000 m	*Saino and Hattori* [1987]
	Sinking particle		
KK1	May 2011	100–150 m	This study
M1S	September 2001 to March 2002	374–2700 m	*Kao et al.* [2012] and this study
M2S	December 2001 to May 2002	447–3250 m	*Kao et al.* [2012] and this study
SEATS	August 2004 to November 2005	200–3500 m	*Liang* [2008]
Central SCS (n = 3)	1992–1999	1200–3750 m	*Gaye et al.* [2009]
Southern SCS (n = 3)	1998–1999; 2003–2006	600–1700 m	*Gaye et al.* [2009]
	Zooplankton		
Northern SCS (n = 5)	July–August 2009	0–100 m	This study
Northern SCS (n = 6)	January 2010	0–100 m	This study
	Fluff Sediment		
Entire SCS basin (n = 32)	2006	–	*Robinson et al.* [2012]
	Surface Sediment		
Entire SCS basin (n = 52)	April–June 1994	–	*Kienast* [2000]

In addition, substantial amounts of allochthonous particles from different origins of sedimentary components can be transported into the deep basin of the SCS [*Kienast et al.*, 2005; *Schroeder et al.*, 2015]. The mixing of allochthonous and autochthonous particles may lead to confounding influences not only on sedimentation rates but also on geochemical proxies in the sediments. It is hence necessary to fully understand the potential mechanisms of N isotopic signatures in POM during settling and burial in the entire water column prior to utilizing sedimentary $\delta^{15}N$ to reconstruct modern and past N cycles.

In this paper, we first report a new data set of $\delta^{15}N$ for the northern SCS, including nitrate, sinking POM from the whole water column, and zooplankton from the EZ. Combined with reported isotopic data of suspended and sinking POM as well as surface sediments (Table 1), we examine the N dynamics of both dissolved and particulate phases from production in the water column to burial in sediments. Carbon isotopic compositions and C/N ratios are also applied to discern the sources of particles. Specifically, we attempt to unravel (1) the transformation of N isotopic signatures among different N pools in the upper water column and (2) the processes involved in changes in the $\delta^{15}N$ values of sinking POM ($\delta^{15}N_{sink}$) in the water column and their implications for the preserved N isotopic record in the sediment. This study may benefit future modern study and paleostudy of the N cycle in the SCS and analogous marginal seas.

2. Methods and Materials

2.1. Sample Collection

2.1.1. Water Samples and Floating Traps

Water samples for nitrate were collected in the northern SCS and WPS off the LS during May 2011 (Figure 1) using a Sea-Bird SBE-911plus CTD-rosette sampling system with 12 L Niskin bottles on board the R/V *Dongfanghong II*. Seawater samples of approximately 100 mL were recovered on 2–3 hydrocasts from surface to bottom and then collected in 125 mL high-density polyethylene (HDPE) bottles which had been soaked in 1 N HCl for 24 h and rinsed with deionized water. Each HDPE bottle was rinsed three times with in situ sample water before being filled. Samples were immediately frozen at −20°C until analysis.

During this cruise, we also deployed an array of floating sediment traps at 100 m and 150 m at the KK1 site (Figure 1) for ~27 h to collect sinking particles. Relatively short deployment time was thought to reduce efficiently the potential solubility and/or decomposition of organic matter within sinking particles,

Table 2. The C/N Ratios and $\delta^{15}N$ Values of Three Net-Plankton Size Fractions in the SCS During July–August 2009 and January 2010[a]

				$\delta^{15}N$ (‰)			C/N (Atomic)		
Site	Latitude [°N]	Longitude [°E]	Season	200–500 (μm)	500–1000 (μm)	>1000 (μm)	200–500 (μm)	500–1000 (μm)	>1000 (μm)
LE05	18.00	114.00	Summer	3.9	5.1	5.5	5.2	4.7	4.9
E607	18.51	114.51	Summer	4.0	4.5	5.5	5.2	4.8	4.9
S504	19.73	117.60	Summer	4.4	5.1	5.9	5.0	4.9	5.2
A10	19.27	116.68	Summer	4.2	5.0	5.9	5.3	5.1	5.1
E406	18.75	120.01	Summer	4.0	4.9	4.7	5.8	5.1	6.0
E607	18.50	114.50	Winter	5.8	6.8	7.8	5.2	4.3	4.3
SEATS	17.99	115.97	Winter	5.0	6.0	5.8	5.3	4.6	4.3
A2	20.47	115.45	Winter	5.2	6.1	7.0	4.8	4.6	4.4
S504	19.73	117.60	Winter	4.7	5.8	6.4	5.2	4.6	4.6
S412	19.77	119.11	Winter	6.1	6.6	6.7	4.7	4.3	4.3
E406	18.76	120.00	Winter	4.3	5.4	5.2	5.2	4.5	4.3

[a]The location of sampling site is shown in Figure 1.

following *Altabet* [1988]. The trap array at each depth contained four cylindrical plastic tubes (with a diameter of 10 cm and length of 50 cm) filled with prefiltered (pore size 0.2 μm) surface seawater with reagent NaCl added at a concentration of 86 g L^{-1}, and with honeycomb baffles placed at the tube mouth. After recovery, the collection tubes were stood at 4°C to allow the particles to settle to the bottom. Then, the upper layer waters were siphoned off and all visible zooplankton in the remaining waters were carefully picked up. Sinking particles were filtered off through a combusted (450°C for 4 h) Whatman 47 mm diameter GF/F membrane and then preserved at −20°C until analysis.

2.1.2. Zooplankton

Samples of zooplankton were collected with a 200 μm mesh size plankton net (with a diameter of 0.5 m) through the upper 100 m of water column in the northern SCS basin onboard the R/V *Dongfanghong II* during July–August 2009 and January 2010 (Figure 1). The information on sampling sites is listed in Table 2. After recovery, zooplankton was separated into three size fractions by passing successively through 200, 500, and 1000 μm Nitex sieves. Then, size-fractioned samples were quickly stored frozen at −80°C on board. Once taken back to the laboratory, the frozen samples were lyophilized and preserved in an autodesiccator until elemental and isotopic analysis.

2.1.3. Time Series Sediment Trap Samples

Time series sediment traps with an aspect ratio of 2.5 and a collection area of 0.125 m^2 (Technicap PPS 3/3, French made) were deployed at ~400–3000 m to collect sinking particles at the M1S site from September 2001 to March 2002, and the M2S site from December 2001 to May 2002 in the northern SCS (Figure 1 and Table 3). The sampling intervals at the two sites were 15 days. Before deployment, all collecting cups were filled with a buffered (5%) formalin solution ($7.5 < pH < 8.0$) to poison "swimmers" and to prevent samples from degradation. The recovered samples were stored at 4°C on board and then taken to the laboratory. Larger particles (mainly including zooplankton and other swimmers) were removed using a Teflon sieve with pore size of 1 mm, and then the remaining visible organisms were picked up. The pretreated samples were filtered through precombusted (500°C for 4 h) and preweighed Millipore membrane filters (47 mm diameter and 0.45 μm pore size) and then rinsed three times with deionized water to remove any salts. The desalted samples were dried at 40°C for 48 h and then weighed again. Detailed information for the pretreatment of sinking particles is given by *Liu et al*., 2007. The total mass flux (TMF) was calculated as follows:

$$\mathrm{TMF} = \left(m_{\mathrm{sample}} - m_{\mathrm{filter}}\right)/(S \times T), \quad (1)$$

where m_{sample} and m_{filter} denote the dry weight of sample with filter and the filter weight and S and T express the collection area of the trap and the duration for each sample collection. After that, they were ground into a fine powder and then stored in a thermostatic vacuum desiccator until analysis.

2.2. Elemental and Isotopic Analysis

To remove carbonates, ~2 mL of 1 N HCl (GR grade) were added to the trap samples, which were subsequently dried at 60°C for 48 h as indicated in prior studies [e.g., *Casciotti et al*., 2008; *Kao et al*., 2012;

Table 3. Sampling Information, Total Mass Flux, Organic Carbon and Nitrogen Contents and C/N Molar Ratio, Flux-Weighted Average $\delta^{13}C$, and $\delta^{15}N$ Values of Sinking Particles

Site	Latitude [°N]	Longitude [°E]	Bottom Depth (m)	Trap Depth (m) (Sampling No.)	Range of TMF (mg m^{-2} d^{-1})	Average TMF (mg m^{-2} d^{-1})	C_{org}%[a]	N%	C_{org}/N[a] (Atomic)	$\delta^{13}C$[a] (‰)	$\delta^{15}N$ (‰)
M1S	21.52	119.46	2943	374 [11]	101.9–613.2	252.8	15.5 ± 4.8	2.5 ± 0.8	7.4 ± 1.2	−22.2	5.2[b]
				925 [10]	122.6–2140.2	457.8	5.0 ± 2.2	0.7 ± 0.3	8.5 ± 1.6	−22.3	4.5
				1925 [12]	227.0–5477.3	1006.2	2.9 ± 1.1	0.4 ± 0.2	8.3 ± 0.4	−22.5	3.6
				2700 [11]	231.4–2172.5	858.2	2.6 ± 0.9	0.4 ± 0.1	8.3 ± 0.5	−22.5	3.4
M2S	19.00	117.49	3743	447 [9]	141.6–1076.9	528.3	40.0 ± 6.1	4.5 ± 1.2	11.2 ± 4.2	−24.3	5.5[b]
				1248 [10]	59.8–390.1	232.3	7.6 ± 2.3	0.9 ± 0.3	9.7 ± 1.6	−23.1	3.4
				3250 [10]	160.0–512.7	318.3	4.6 ± 0.6	0.6 ± 0.1	9.3 ± 1.0	−23.2	3.2
KK1	17.98	115.98	3874	100 [2]	-	741.2	16.7	2.4	7.6	−23.5	4.9
				150 [2]	-	641.2	9.2	1.1	8.9	−24.6	3.3

[a]The data are derived from *Liu et al.* [2007].
[b]The values are reported by *Kao et al.* [2012].

Loick et al., 2007]. Approximately 2–15 mg of the decarbonated samples were transferred to tin capsules, while samples of size-fractioned zooplankton were transferred to tin capsules without acid treatment and delipidation. Afterward, we analyzed C/N contents, and their isotopic compositions using a continuous flow system with an elemental analyzer (Carlo-Erba EA 2100) connected to an isotope ratio mass spectrometer (IRMS, Thermo Finnigan Delta^{plus} Advantage) system. In each batch, international (USGS 40, L-glutamic acid with $\delta^{15}N$ of -4.5 ± 0.1‰) and working (acetanilide with $\delta^{15}N$ of -1.5 ± 0.2‰, Merck) standards were inserted into every five to six samples for calibration. Isotopic compositions are expressed in δ notation as follows:

$$\delta X\ (‰) = \left[\left(R_{sample}/R_{standard}\right)-1\right] \times 1000, \quad (2)$$

where X shows ^{13}C or ^{15}N and R is the $^{13}C/^{12}C$ or $^{15}N/^{14}N$. The long-term reproducibility of C and N isotopic compositions for standards and field samples in our laboratory was better than 0.2‰.

The concentrations of nitrate plus nitrite ($[NO_3^- + NO_2^-]$ and $[NO_2^-]$) were determined on board using a Technicon AA3 Auto-Analyzer (Ban-Lube, GmbH) with standard colorimetric methods following *Du et al.* [2013]. The detection limits for nitrate plus nitrite and nitrite were 0.07 μM and 0.03 μM, respectively. Nitrite concentration was under the detection limit below 100 m and its content was generally less than 10% in the EZ when the samples used for isotope measurement had $[NO_3^- + NO_2^-] > 0.5$ μM. Note that hereafter $[NO_3^- + NO_2^-]$ is reported as $[NO_3^-]$, and nitrite was not removed or measured separately for isotopic composition [*Granger and Sigman*, 2009].

Measurements of $\delta^{15}N_{NO3}$ followed the "denitrifier method" first reported by *Sigman et al.*, 2001. Briefly, a strain of denitrifying bacteria lacking nitrous oxide (N_2O) reductase activity was used to quantitatively convert sample nitrate plus nitrite (10 or 20 nmol in routine measurements) into N_2O. Then, isotopic analysis of the produced N_2O was conducted using a continuous flow Gasbench II-IRMS system. The measured $\delta^{15}N_{NO3}$ values were standardized using four international NO_3^- isotopic references, International Atomic Energy Agency-N3 with a $\delta^{15}N_{NO3}$ of 4.7‰, U.S. Geological Survey (USGS) 34 with a $\delta^{15}N_{NO3}$ of −1.8‰, USGS 35 with a $\delta^{15}N_{NO3}$ of 2.7‰, and USGS 32 with a $\delta^{15}N_{NO3}$ of 180‰. In terms of sample replicates, the standard deviation for $\delta^{15}N_{NO3}$ measurement was less than 0.2‰, similar to that in prior studies [e.g., *Yang et al.*, 2014].

3. Results

3.1. Nitrate Concentration and Its N Isotope in the Northern SCS

In general, the nitracline depth (NTD, defined as the depth with $[NO_3^-] > 0.1$ μM) was at the depth of ~50–75 m in the northern SCS (Figure 2), shallower than that in the WPS (125–150 m). Below the nitracline, $[NO_3^-]$ in the SCS continuously increased downward reaching ~38.5 μM when below 2000 m. In the WPS, $[NO_3^-]$ increased to ~39.0 μM at ~1200–1300 m and then decreased slightly to ~36.1 μM below 4000 m. Compared to those in the WPS, the $[NO_3^-]$ at sites in the northern SCS were quite higher in the upper 600 m, but slightly lower at ~600–2500 m (Figure 2).

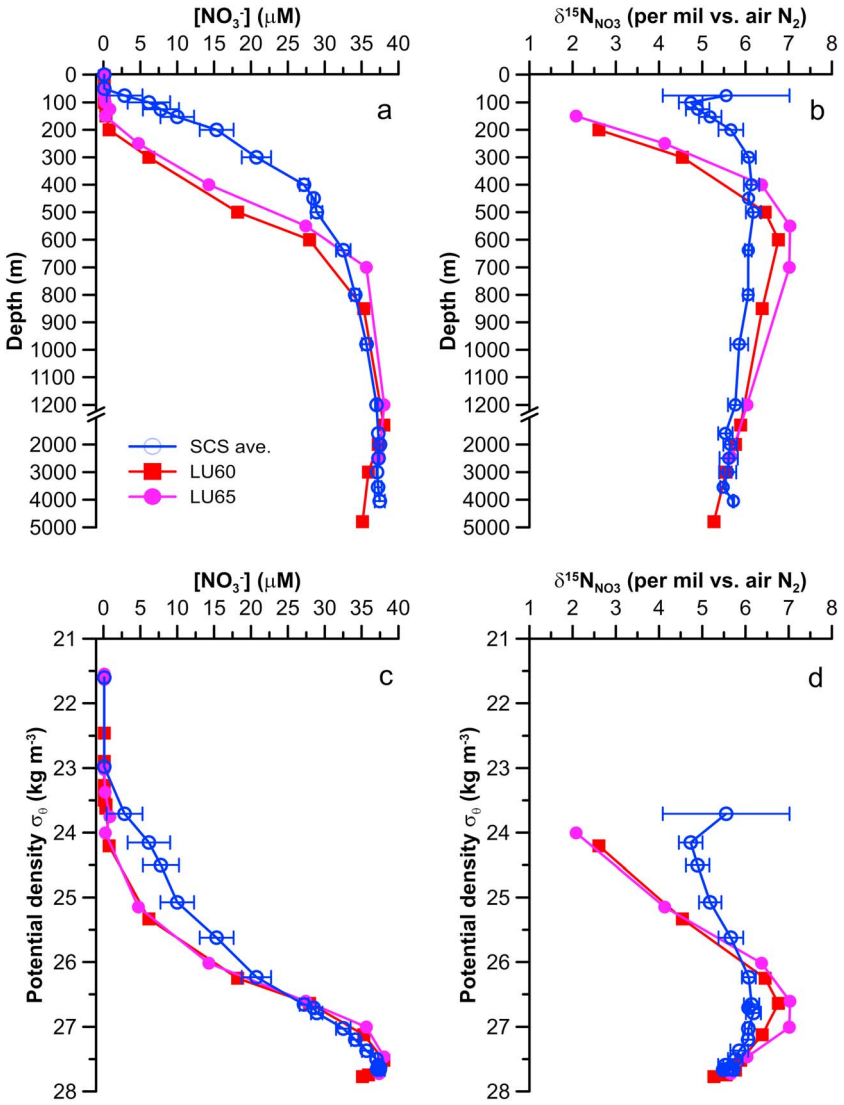

Figure 2. Depth and isopycnal profiles of (a and c) $[NO_3^-]$ and (b and d) $\delta^{15}N_{NO3}$ in the northern SCS and WPS. Note that the profiles of $[NO_3^-]$ and $\delta^{15}N_{NO3}$ for all sites in the northern SCS are shown as the average values (±1 SD) since their distributions are very comparable. The locations of all sites are shown in Figure 1.

The $\delta^{15}N_{NO3}$ values below 2000 m in the northern SCS and WPS were ~5.2–5.7‰. An upward increasing pattern of $\delta^{15}N_{NO3}$ was found from deep to intermediate waters, showing maxima of ~6.0‰ at 300–500 m in the northern SCS and ~7.0‰ at 500–600 m in the WPS. The $\delta^{15}N_{NO3}$ maxima in the SCS and WPS were located at similar potential density surfaces (σ_θ = ~26.5–26.8) and fell within the salinity minimum associated with the NPIW though with different water depths. In waters above the intermediate water, the $\delta^{15}N_{NO3}$ displayed subsurface minima both in the northern SCS and WPS at similar σ_θ surfaces. The $\delta^{15}N_{NO3}$ minima in the WPS were ~2.1–2.6‰ at 150–200 m, which were ~2.5‰ lower than those at ~100–125 m in the northern SCS. Around the NTD and above (Figures 2a and 2b), we found ^{15}N enrichments from the lower EZ toward the surface, which was primarily attributed to a preferential uptake of lighter N by the phytoplankton (generally with an isotopic fractionation effect of ~5‰ [e.g., *Altabet*, 2001]).

3.2. Isotopic Compositions and C/N Ratios of Zooplankton in the Northern SCS

The C/N ratios and N isotopic compositions of the zooplankton for three size fractions (200–500, 500–1000 and >1000 μm) collected during summer and winter in the northern SCS are presented in Table 2. The C/N ratios of size-fractioned zooplankton overall varied in a narrow range from 4.3 to 6.0 without any apparent seasonal pattern.

N isotopic compositions of zooplankton ($\delta^{15}N_{zoo}$), overall ranged from 3.9‰ to 7.8‰. The average $\delta^{15}N_{zoo}$ values generally increased on average by ~0.7‰ with each size fraction at the observed sites in the northern SCS, varying between 4.1 ± 0.2‰ and 5.5 ± 0.5‰ in summer, and between 5.2 ± 0.7‰ and 6.5 ± 0.9‰ in winter (Table 2). Compared to those in summer, relatively higher $\delta^{15}N_{zoo}$ values were observed in winter for the 200–500 and 500–1000 μm size fractions, while no significant seasonal difference was presented for >1000 μm size fraction ($p > 0.05$). A similar difference in the $\delta^{15}N$ of suspended POM ($\delta^{15}N_{sus}$) was also reported between summer and winter, being attributed to the deepening of the mixed layer in winter [*Kao et al*., 2012]. This suggested that changes in $\delta^{15}N$ of the food (i.e., suspended POM) could probably have led to the seasonal variation of $\delta^{15}N_{zoo}$.

3.3. Fluxes and Isotopic Compositions of Sinking Particles in the Northern SCS

3.3.1. Shallow Sinking Particles Collected With Floating Traps

The average $\delta^{15}N_{sink}$ values observed near the bottom of the EZ at the KK1 site were ~4.9‰ at 100 m and ~3.3‰ at 150 m. Also, the $\delta^{15}N_{sink}$ values were similar to the $\delta^{15}N$ values in the subsurface nitrate (4.8 ± 0.3‰), and in sinking POM (5.3 ± 1.3‰) collected using mooring traps at 300–500 m in the northern SCS [*Kao et al*., 2012]. The TMF spanned 641.2–741.2 mg m^{-2} d^{-1} at 100–150 m. In addition, the C/N ratios ranged from 7.6 to 8.9, while the $\delta^{13}C$ values varied between −24.6‰ and −23.5‰ (Table 3). These values fell within the range of suspended POM observed in the upper 200 m at the same site, suggesting the dominance of marine-derived POM [*Liu et al*., 2007].

3.3.2. Deep Sinking Particles Collected by Mooring Traps

Figure 3 shows a time series of TMF, PN fluxes (PNF), $\delta^{15}N$, and N contents (N%) of the sinking particles at different depths at the M1S and M2S sites. Overall, the TMF of sinking particles at the two sites between September 2001 and May 2002 varied within a large range, from 59.8 to 5477.3 mg m^{-2} d^{-1}. The seasonal pattern of TMF showed higher values from winter to early spring (December–March) and lower in autumn (September–November) and late spring (April–May). Furthermore, it is worth noting that the TMF collected in the deep traps (~2000–3000 m) were considerably higher than those in upper ones, especially at the M1S site (Figure 3 and Table 3) where the TMF was ~10 times higher during winter.

The PNF in the upper traps (374–447 m) spanned 2.9–66.6 mg N m^{-2} d^{-1} (data reported in *Kao et al*. [2012]), revealing a similar temporal trend relative to the TMF (Figure 3). Furthermore, the PNF in the upper traps at the M2S site were higher than those at the M1S site primarily due to relatively higher N% (Figure 3 and Table 3) despite the fact that the corresponding deployed depth at the M2S site was deeper. Narrow ranges of PNF were observed in the lower traps (925–3250 m) at both sites, varying from 0.7 to 12.2 mg N m^{-2} d^{-1} with an average of 2.5 ± 1.9 mg N m^{-2} d^{-1} with no clear seasonal variations. Nevertheless, higher PNF values could still be found in the deep traps during the time intervals with considerably high TMF. In addition, N% in the upper traps (2.5–4.5%) were substantially higher than those (~0.5%) below ~2000 m (Table 3), showing a weak minimum in winter.

The $\delta^{15}N_{sink}$ values in the upper traps showed flux-weighted averages of 5.2‰ and 5.5‰ at the M1S and M2S sites, respectively, displaying higher values in winter and early spring [*Kao et al*., 2012]. Below 1000 m, the $\delta^{15}N_{sink}$ values presented a roughly similar temporal trend, but within narrower ranges. However, there were significant decreases in $\delta^{15}N_{sink}$ in the deep traps with flux-weighted averages of ~3.2–3.6‰ at ~3000 m ($p < 0.05$). The potential mechanisms of such decreases in $\delta^{15}N_{sink}$ will be discussed later.

4. Discussion

4.1. Transformation of N Isotopic Signals in the Upper Layer of the SCS

In order to reveal N isotopic endmember of new N and N isotope transfer among different N pools in the upper water column of the SCS, we examine a new data set of $\delta^{15}N$ in the zooplankton from the EZ, nitrate, and sinking POM collected using floating traps in the upper 150 m and also compare this with all reported $\delta^{15}N$ values in suspended particles in the EZ. Sinking particles recovered using mooring traps at 200–500 m from previous studies in the SCS are compiled for discussion (Table 1 and Figure 4). We note that all data sets used in this study are collected in a long-time frame of over 10 years. However, the $\delta^{15}N$ values recorded in the coral skeleton in the northern SCS showed minor changes (±0.7‰) over the past 45 years

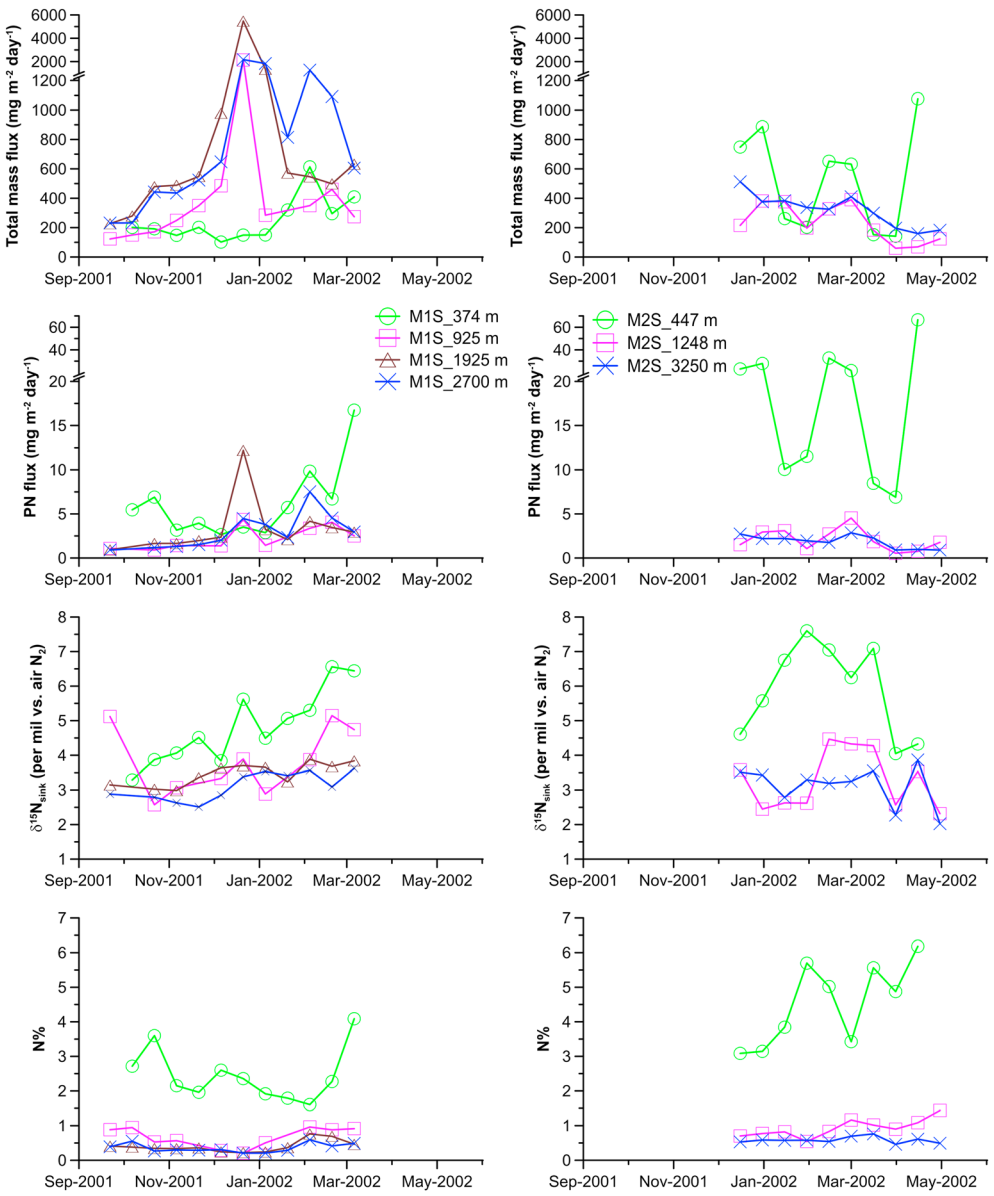

Figure 3. Time series of total mass and PN fluxes, δ^{15}N values, and nitrogen contents (N%) of sinking particles collected at different depths of the (left column) M1S and (right column) M2S sites.

[*Ren et al.*, 2017]. This suggests that the influence of the time lag of sampling collection on the δ^{15}N background is limited.

We first examine spatial-temporal patterns of $\delta^{15}N_{NO3}$, which could determine the POM δ^{15}N exported from the EZ (Figure 2). The $\delta^{15}N_{NO3}$ values below 2000 m in the northern SCS and WPS were 5.2–5.7‰, which are identical to those (5.4 ± 0.2‰) in the deep North Pacific [e.g., *Casciotti et al.*, 2008] and slightly higher than the global mean δ^{15}N value of deep ocean nitrate (4.8 ± 0.2‰ below 2.5 km [*Sigman et al.*, 2000]). Intermediate $\delta^{15}N_{NO3}$ maxima found at similar σ_θ surfaces are likely attributed to heterotrophic denitrification in the oxygen minimum zone of the ETNP and then imported by the NPIW to the west as indicated by previous modern and paleostudies [*Kao et al.*, 2008; *Liu et al.*, 1996; *Rafter et al.*, 2012; *Sigman et al.*, 2009]. The distribution of $\delta^{15}N_{NO3}$ in the northern SCS presented minimum values of 4.8 ± 0.3‰ (n = 14) in the subsurface (~100–125 m; Figure 2). This is a common pattern observed in other tropical and subtropical oligotrophic oceans, primarily as a result of the accumulation of lighter N signals (^{14}N-enriched) from the atmosphere (e.g., N_2 fixation and atmospheric N deposition) and preferential remineralization of low δ^{15}N organic

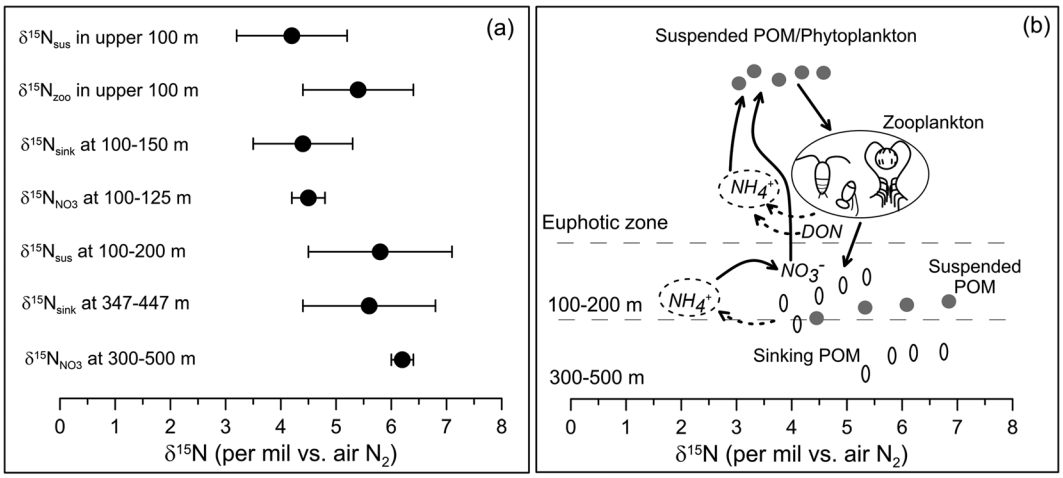

Figure 4. Comparison of average $\delta^{15}N$ values (±1 SD) among (a) different N pools and (b) schematic diagram of N transformation in the upper 500 m of the SCS. The solid and open symbols indicate the suspended and sinking POM and correspond to the value ranges as seen in Figure 4a. Zooplankton and their isotopic value range are also shown. The positions of the dissolved phases (NO_3^-, DON, and NH_4^+) correspond to their average isotopic values shown in Figure 4a for each depth interval.

matter [e.g., *Bourbonnais et al*., 2009; *Casciotti et al*., 2008; *Kao et al*., 2012; *Liu et al*., 1996; *Yang et al*., 2014]. In addition, it is in line with the only $\delta^{15}N_{NO3}$ profile with a subsurface minimum of 4.6 ± 0.2‰ observed at the SEATS site during April 1997 [*Wong et al*., 2002]. Such a consistency suggests that vertical patterns of $\delta^{15}N_{NO3}$ in the SCS basin might not change in different years. However, additional data are needed to investigate the seasonal variation of $\delta^{15}N_{NO3}$ in the future. The $\delta^{15}N_{NO3}$ profiles in the SCS interior are found to be spatially uniform (Figure 2), implying dynamically and rapidly isopycnal and diapycnal mixings as indicated previously [*K. K. Liu et al*., 2010]. A contrasting pattern of $\delta^{15}N_{NO3}$ profiles in the WPS is observed although the northern SCS is characterized as a region of intense communication with the open WPS via the LS.

The ^{15}N-depleted signals found in the WPS subsurface are most likely due to the effect of N_2 fixation since high rates of nitrogen fixation and high abundance of diazotrophs in the West Pacific have been reported previously [*Chen et al*., 2008; *Shiozaki et al*., 2010]. The $\delta^{15}N_{NO3}$ minimum in the northern SCS near the LS may be influenced by the isopycnal mixing when the Kuroshio intrusion intensifies. However, the low $[NO_3^-]$ (<1 μM) at the $\delta^{15}N_{NO3}$ minimum in the WPS prohibits significant alteration on the $\delta^{15}N_{NO3}$ minimum (with $[NO_3^-]$ of >5 μM; see Figure 2) in the northern SCS. By assuming that the $[NO_3^-]$ of upwelled water has the same value as those in the observed subsurface (in fact, nitrate is higher in deeper water), a simple two-end-member mixing model suggests that the mixing from the WPS could lower the $\delta^{15}N_{NO3}$ values in the subsurface by 0.2–0.3‰ at most. Furthermore, lower $\delta^{15}N_{NO3}$ values (2–4‰) in the subsurface have been reported for the southwestern SCS [*Loick et al*., 2007] where the Kuroshio influence is obviously insignificant. Thus, the influence of isopycnal mixing with the WPS is limited.

The shallow NTD in the SCS basin (~50–75 m, Figure 2a), maintained by the cyclonic circulation pattern [*You et al*., 2005, and references therein], also implies that nitrate as new N could be supplied steadily from the subsurface into the EZ [*Mino et al*., 2002]. Instead of using 3.3‰ reported in the WPS subsurface as an isotopic endmember for the exported POM in the SCS basin proposed by *Gaye et al*. [2009], we suggest using this newly reported $\delta^{15}N_{NO3}$ of 4.8 ± 0.3‰. The consistent $\delta^{15}N$ values (~4.6‰) between subsurface nitrate and sinking POM collected at 100–150 m in the northern SCS further support our notion. Moreover, the comparable mean $\delta^{15}N_{sink}$ values (4.6 ± 0.8‰, $n = 12$) were reported from long-term mooring traps deployed (~8 months) at 200 m of the KK1 site [*Liang*, 2008]. This is again supportive of the importance of upwelled nitrate for export production in the SCS. In contrast, the $\delta^{15}N_{NO3}$ values of 2.1–2.6‰ in the WPS subsurface were substantially lower ($p < 0.05$, Figure 2) than the mean $\delta^{15}N_{sink}$ values according to this new data set. Judged by the similarity in $\delta^{15}N$ values between shallow sinking POM and subsurface nitrate, the new N from the atmospheric deposition or N_2 fixation is of minor significance [*Kao et al*., 2012; *Yang et al*., 2014], yet its importance is evident as the long-term cumulative signal of lighter N may be responsible for the $\delta^{15}N_{NO3}$

minimum in the subsurface. More studies are needed to explore the nitrogen dynamics in the upper ocean with the strong interplay between physical and biological processes.

It is noteworthy that the average $\delta^{15}N_{sink}$ value (4.4‰) exported out of the EZ is similar to the reported $\delta^{15}N_{sus}$ in the upper 100 m at the SEATS site (an annual concentration-weighted mean of 4.2 ± 1.0‰) [*Kao et al*., 2012] and slightly lower than the annual average $\delta^{15}N_{zoo}$ values (5.4 ± 1.0‰) observed throughout the study area (Figure 4). This phenomenon is uncommon when compared with most tropical and subtropical oligotrophic oceans. In tropical and subtropical oligotrophic regions, the $\delta^{15}N_{sus}$ values (−1–2‰) observed in the EZ are generally significantly lower than the $\delta^{15}N_{sink}$ values exported from the EZ and the $\delta^{15}N_{zoo}$ values [*Altabet*, 1988; *Montoya et al*., 2002; *Saino and Hattori*, 1987]. The relatively low $\delta^{15}N_{sus}$ values have been largely attributable to the recycling of excreted NH_4^+ from the zooplankton and/or inputs of new N from the atmosphere, which can lead to ^{15}N-depleted signals being retained in the EZ. In fact, the *f* ratios (nitrate-based new production/primary production) in the northern SCS were reported to be ~0.2–0.3 [*Chen*, 2005], indicating that the recycled N must play a role in supporting PN production. If the reported low *f* ratios are correct, conflicts thus appear to maintain such a small difference in $\delta^{15}N$ between suspended and sinking POM in the EZ under the condition of high regenerated production. The only way to maintain such an isotope balance is that the $\delta^{15}N$ values of recycled N (e.g., NH_4^+ and urea) are close to those of new N (e.g., subsurface NO_3^-). Otherwise, the reported *f* ratios are to be questioned.

The most likely source to refuel NH_4^+ is the dissolved organic nitrogen (DON) pool, which is generally 10 times higher than the PN pool in terms of concentration and has a steady isotopic composition of ~5‰ in the North Pacific [e.g., *Knapp et al*., 2011]. The DON in the oligotrophic region is mineralized rapidly by upper mesopelagic bacterioplankton [*Letscher et al*., 2013]. The characteristics of regional and basin-wide upwelling in the SCS could benefit from the utilization of surface DON transported from the WPS via the Kuroshio intrusion [*Wu et al*., 2015]. If this mechanism is correct, the DON supply from the WPS could be critical to maintain primary productivity in the SCS, yet its contribution is undetectable in terms of isotopic composition. On the other hand, a recent study revealed that besides NH_4^+, other small organic N compounds, e.g., urea, played an important role in making up the significant shortage for primary productivity in the SCS [*Dong et al*., 2010]. The narrow $\delta^{15}N$ range between suspended and sinking POM is in line with the observations conducted in the equatorial upwelling regions of the tropical Pacific Ocean [*Altabet*, 2001] and the areas with the occurrence of cyclonic eddies [e.g., *Mahaffey et al*., 2008] where NO_3^- and bacterioplankton from the deep ocean can be readily injected into the surface by physical processes. All aforementioned evidences point to rapid N turnover in the ecosystem.

In fact, our isotopic data of zooplankton could also provide an evidence to support the hypothesis of rapid turnover of N in the northern SCS. The observed increase in $\delta^{15}N_{zoo}$ with size fraction was on average ~0.7‰ (Table 2). Similar increases in $\delta^{15}N_{zoo}$ have also been reported in the Vietnamese upwelling area (southwestern SCS) [*Loick et al*., 2007] and other oligotrophic oceans [e.g., *Hannides et al*., 2013; *Koppelmann et al*., 2009]. Such an isotope increment is significantly lower than the generally reported enrichment of $\delta^{15}N$ (~3.5‰) between trophic levels [*Montoya et al*., 2002], indicating that different size fractions of zooplankton in the EZ may occupy the same trophic level. Since the average $\delta^{15}N_{zoo}$ values are nearly equivalent to or slightly higher (within 1‰) than the $\delta^{15}N_{sink}$ values obtained at 100–200 m ($p < 0.05$), the ^{15}N–enrichment due to trophic processes is ineffective in the SCS basin. Although the mechanisms cannot be resolved by this study, our evidences together indicate that the trophic associated processes may excrete NH_4^+ with similar $\delta^{15}N$ values of upwelled new N. Alternatively, the regenerated production supported by excreted NH_4^+ plays a minor role compared to that maintained by the DON supply and/or new production as mentioned above. Note that if the previously reported *f* ratios are correct, then the isotopic fractionation factor during ammonium excretion remains unresolved. More studies should be done to reevaluate the relative importance of new and regenerated production and to explore complicated N transformation processes among dissolved and particulate pools in terms of isotopic perspective.

4.2. Vertical Distribution of PN Fluxes and $\delta^{15}N$ Values in Sinking POM

As stated earlier, the $\delta^{15}N_{sink}$ values exported out of from the EZ can reflect isotopic signals of new N in the SCS. However, how these isotopic signals transfer downward in the water column remains unclear. In this

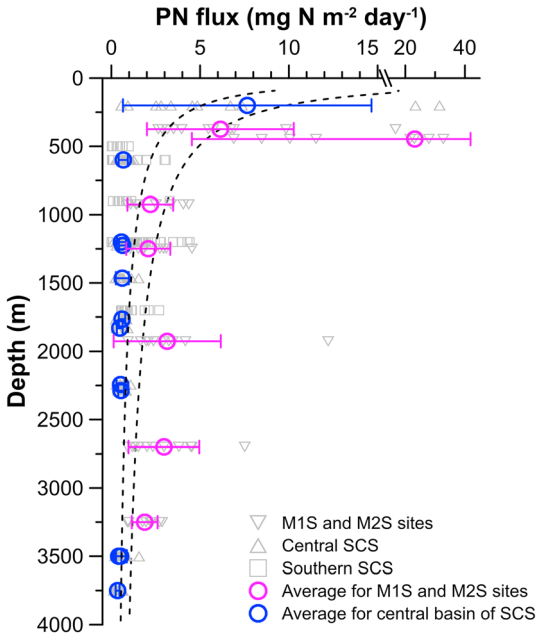

Figure 5. Vertical distribution of PN fluxes in the SCS. The observed average values for each depth are shown in colored symbols. Simulated profiles of PN flux (dashed curves) are based on the Martin curve as $F_{EX}(Z) = F_{Z0}(Z/Z_0)^{-b}$, where Z is the trap depth, $F_{EX}(Z)$ and F_{Z0} denote the PN fluxes at trap depth and from the EZ (here Z_0 is the depth of ~92 m), and b (0.76) is a unitless factor determining the degraded degree of POM with depth. Export production is assumed to be 9.2–17.8 mg N m^{-2} d^{-1} [*Wong et al.*, 2007].

section, we discuss the vertical distribution of the $\delta^{15}N_{sink}$ values from their departure out of the EZ to their deposition in the sediments, and also the potential mechanisms for their alteration.

4.2.1. Vertical Distribution of Total Mass and PN Fluxes Throughout the Water Column

Substantially high TMF were observed in the deep waters (>900 m), especially at the M1S site near Kaoping Canyon (Figure 3 and Table 3). *Chung et al.* [2004] also observed such a downward increasing pattern of TMF in the same area although their values were slightly lower than our results. In fact, similar phenomena were reported in the central (the SEATS, SCS-NE, SCS-NC, and SCS-C sites) and southern (the SCS-SW, SCS-SC, and SCS-S sites) SCS basins (see Figure 1) [*Gaye et al.*, 2009; *Lahajnar et al.*, 2007; *Schroeder et al.*, 2015]. Moreover, there is no consistency in the seasonal pattern at different depths from subsurface to deep waters in our study regions (Figure 3), as well as in the central SCS basin reported by *Gaye et al.* [2009]. The average TMF in the deep waters of the northern basin are 3–5 times higher relative to those in the central basin, implying that particulate materials might have been laterally transported from the shelf and slope. This nonvertical process is basin wide and could have been a potential contributor of organic components to the deep waters.

To evaluate the contribution of lateral transport to the PNF in the SCS basin, all data sets of the PNF from previous and present studies are combined for comparison (Figure 5). Theoretically, vertical distribution of the PNF is controlled both by export production and POM degradation during settling, generally showing an exponential decrease with depth [e.g., *Martin et al.*, 1987]. The PNF in the central SCS basin show a similar pattern compared to the simulated values. However, the PNF present higher values below ~2000 m at the M1S and M2S sites than those in the upper layers (~1000 m) and are also 3–6 times higher than those at corresponding depths in the central basin (Figure 5). In addition, the observed PNF in the northern and southern SCS basins show relatively high values compared to the simulated results from the Martin curves. Thus, the input of allochthonous PN may account for the spatial variation and higher values of the PNF observed in the deep waters.

We note that allochthonous PN occurred mostly in the intermediate water (447 m) at the M2S site, and in the deep waters (2000–3000 m) at both sites (Figure 5). Based on the discrepancy between the observed and simulated values, allochthonous PN could be estimated to supply at least ~80% PNF in the intermediate waters and 45–54% in the deep waters. Such high amounts of POM might be associated with particles being laterally transported from nearby submarine canyons or high productive shelf. For example, *Huh et al.* [2009] reported that the particle load from the Kaoping River in southwest Taiwan was estimated as 36–49 megaton yr^{-1}, of which ~85% was transported to the SCS deep basin via the Kaoping Canyon.

4.2.2. Potential Sources of Allochthonous PN

Lateral advection of allochthonous PN ocurred at different depths of the M1S and M2S sites, implying that various origins might exist to sustain the nepheloid layers in the intermediate and deep waters. In order to

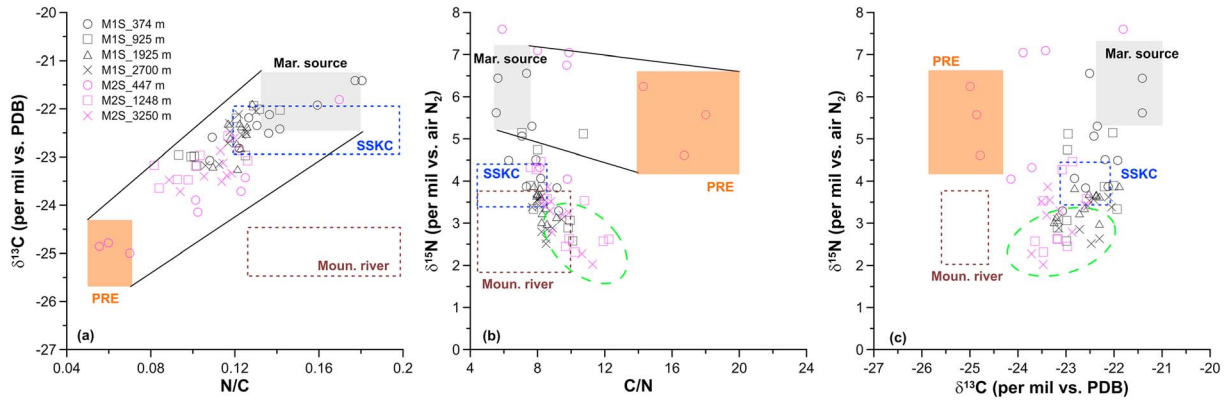

Figure 6. Scatterplots of (a) $\delta^{13}C$ values versus N/C ratios, (b) $\delta^{15}N$ values versus C/N ratios, and (c) $\delta^{13}C$ values versus $\delta^{15}N$ values in sinking particles. The end-members of sinking POM from marine source (Mar. source), Pearl River estuary (PRE), and mountainous river (Moun. river), as well as surface sediments around the Kaoping Canyon (SSKC) are marked (Table 4). The mixing curves for the end-members of sinking POM from marine and the Pearl River estuarine sources are shown in Figures 6a and 6b. The green dashed ellipses in Figures 6b and 6c indicate the sinking particles in the deep waters with lower $\delta^{15}N$ values possibly due to microbial activities and/or selective export of picoplankton (see text).

better constrain the potential sources of allochthonous PN, we combine the N isotope with the C isotope and C/N ratio of the sinking POM from this study area for discussion (Figure 6).

The isotopic and elemental end-members of potential sources for sinking POM in the northern SCS (including marine and the Pearl River estuary and mountainous river (from Taiwan and Luzon) sources, as well as surface sediment from the Kaoping Canyon) are summarized in Table 4. Overall, sinking POM from the upper water column to the deeper waters is characterized as a mixture of marine and the Pearl River estuarine sources based on the relationship between the $\delta^{13}C$ value and the N/C ratio (Figure 6a), similar to that proposed by *Liu et al.* [2007]. Significant contributions from the Pearl River estuary are found specifically at 447 m of the M2S site (Figure 6a). The particles from the Pearl River estuary with relative high $\delta^{15}N$ values (4.6–6.2‰), as shown in Figure 6b, are likely the reworked POM composed of soil-derived terrestrial and in situ produced sources [*Hu et al.*, 2006; *Zhang et al.*, 2014]. They can be buried in the sediments on the continental shelf temporally and then resuspended and exported seaward in winter [*Liu et al.*, 2007].

Remarkably, most data fall below the mixing curves of the marine and the Pearl River estuarine sources mainly due to relatively low $\delta^{15}N_{sink}$ values (Figure 6b). Low $\delta^{15}N_{sink}$ values at 374–447 m can primarily be interpreted by the contribution of external N from the atmosphere during spring and autumn, most of which recycles in the subsurface waters [*Kao et al.*, 2012]. The ^{15}N-depleted signals of external N from the atmosphere that sink into the depth could be thus negligible, which have an insignificant influence on the reduction in $\delta^{15}N_{sink}$ in the deep waters. Together with the higher PNF, the lower $\delta^{15}N$ and C/N ratios of sinking POM observed in the deep waters imply that the POM from the Pearl River estuary have been diluted by lateral-derived POM from other marginal areas. Mountainous rivers could have a substantial contribution to particles settling in the SCS deep basin during extreme events as reported previously (e.g., typhoons [*Kao et al.*, 2010; *Selvaraj et al.*, 2015]). During the study period (September–May), these fluvial particles contribute insignificantly judged by the mixing plot of $\delta^{13}C$-N/C in Figure 6a.

We also find that the $\delta^{15}N$ and $\delta^{13}C$ values in sinking POM tend to be uniform in the deep waters, reaching 3.5 ± 0.2‰ and −22.3 ± 0.2‰, respectively, when the TMF reached its maximum (Figure 3 and Table 3). The isotopic indicators point to an endmember of surface sediment around the Kaoping Canyon (SSKC, Table 4),

Table 4. Elemental and Isotopic End-Members of Sinking POM in the Northern South China Sea

Endmember	C_{org}/N (Atomic)	$\delta^{13}C$ (‰)	$\delta^{15}N$ (‰)	References
Marine source	6.6 ± 1.0	−21.9 ± 0.6	6.2 ± 1.0	*Liu et al.* [2007] and *Kao et al.* [2012]
Pearl River estuary	14–20	−25.0 ± 0.7	4.2–6.6	*Gaye et al.* [2009], *Hu et al.* [2006], *Liu et al.* [2007], and *Zhang et al.* [2014]
Mountainous river	4.4–8	−25.0 ± 0.5	1.8–3.8	*Gaye et al.* [2009] and *Kao et al.* [2006]
SSKC	4.2–8.4	−22.5 ± 0.5	3.4–4.4	*Kao et al.* [2006] and *Yang et al.* [2017]

which is verified to be a mixture of marine primary production and Taiwanese river inputs [*Kao et al*., 2006]. Thus, from isotopic mixing plots we conclude that the SSKC is the most likely source of POM transported laterally to the SCS deep basin by deep contour current and possibly mesoscale eddies [*Z. F. Liu et al*., 2010; *Liu et al*., 2016; *Schroeder et al*., 2015]. Note that some data points apparently fall out of the mixing field with known endmembers in Figure 6b and these samples point toward higher C/N ratios and lower $\delta^{15}N$ values, which are very likely terrigenous organics in/on surface soil. The data from northern Taiwan showing $\delta^{15}N$ of −4.7–0‰ and C/N ratio of 14–36 for soil and vegetation [*Kao and Liu*, 2000] support this notion. Unfortunately, no isotopic data for vegetation and surface soil from southern Taiwan are documented. Thus, the end-members of plant debris and surface soil from Taiwan are not added into mixing plots, yet these sources cannot be excluded.

4.2.3. Influences of Lateral Input on Sediment Accumulation and $\delta^{15}N_{sink}$ Values in the Deep Waters

Since more than 50% of PNF in the deep waters was supplied by allochthonous PN from the SSKC, it could significantly affect the N accumulation rate (AR_N) in the sediments. To assess this influence, we use an empirical equation applied from the shelf off southwestern Taiwan to the downslope from *Kao et al*. [2006]:

$$AR_N = 290 \times D_{bot}^{(-1.2)} \times N\%, \tag{3}$$

where D_{bot} refers to bottom depth. The measured N% values in the surface sediments were 0.14–0.20% near our study area [*Kienast*, 2000]. Given that D_{bot} spanned 3000–4000 m, we could obtain an AR_N of 0.5–1.1 mg N m^{-2} d^{-1}. This estimate suggests that ~22–45% of PNF observed in the deep traps are preserved in the surface sediments, which are significantly higher than the preserved efficiency of organic matter for other SCS regions (10–20%) [*Lahajnar et al*., 2007] and other open oceanic sites (typically 2–10% [*Freudenthal et al*., 2001]). Furthermore, we estimate that ~4–9% of average exported PN from the EZ (~12.3 mg N m^{-2} d^{-1}) is deposited in the sediments. This is also substantially higher than those estimated in the central SCS basin (~1%) [*Wong et al*., 2007].

It is thus conceivable that the impacts of lateral particle advection should also bias the isotopic records of sinking particles and sediments. The $\delta^{15}N_{sink}$ values in the deep waters are assumed to be determined only by the POM $\delta^{15}N$ from local (δ_{local}) and allochthonous (δ_{allo}) sources, and changes of δ_{local} and δ_{allo} during settling and transport could be neglected. A simple two-end-member mixing model is used to calculate the theoretical $\delta^{15}N_{sink}$ values (δ_{theo}) of the mixture, which can be expressed as a function of the fraction of allochthonous PN (f) as follows:

$$\delta_{theo} = f \times \delta_{allo} + (1-f) \times \delta_{local}, \tag{4}$$

where δ_{local} is the observed mean $\delta^{15}N_{sink}$ value of the shallow trap at the M1S site (5.2‰ at 347 m), where the influence of lateral advection was minor, and δ_{allo} is set using the SSKC (3.4–4.4‰). The f is chosen as the average estimate of 45–54% (see above). Thus, δ_{theo} is calculated to be 4.2–4.8‰. These theoretical values are significantly higher than the observed $\delta^{15}N_{sink}$ values in the deep traps (3.2‰), suggesting that other mechanisms may have lowered the $\delta^{15}N_{sink}$ during downward transit.

Combining all the $\delta^{15}N_{sink}$ data in the SCS basin, we find spatially consistently lower $\delta^{15}N_{sink}$ values in the deep waters relative to those in the upper water column over the entire basin even in the central SCS basin where lateral transport is insignificant (Figure 7). There must be some mechanisms to support such a basin-wide downward decreasing trend in $\delta^{15}N_{sink}$. Similar decreasing patterns were reported elsewhere when and/or where export fluxes are relatively low [e.g., *Altabet et al*., 1991; *Nakatsuka et al*., 1997], yet the mechanisms are still under investigation to date. Two potential factors have been proposed: (1) preferential decomposition of the ^{15}N-enriched components or (2) incorporation of light-N species (e.g., NH_4^+) within bacterial biomass. ^{15}N-enriched components are mainly sourced from animals of higher trophic levels (e.g., fecal pellet and marine snow) [*Montoya et al*., 2002], which have relatively higher $\delta^{13}C$ values in general [*Hannides et al*., 2013]. Thus, the loss of ^{15}N-enriched components may accompany the loss of ^{13}C. However, the $\delta^{13}C$ values of sinking POM were statistically unchanged throughout the water column (Table 3); thus, preferential decomposition is unlikely. Recent studies related to measurements of $\delta^{15}N$ in specific AA compounds demonstrated that heterotrophic microbial reworking of proteinaceous material can resynthesize and salvage AA into new proteins, and change the $\delta^{15}N$-AA pattern in sinking POM [*McCarthy et al*., 2007]. Whether this process may simultaneously alter the $\delta^{13}C$ remains unknown, influences of microbial activities on dual isotopes of bulk POM and organic compounds at depth need to be further explored in the future.

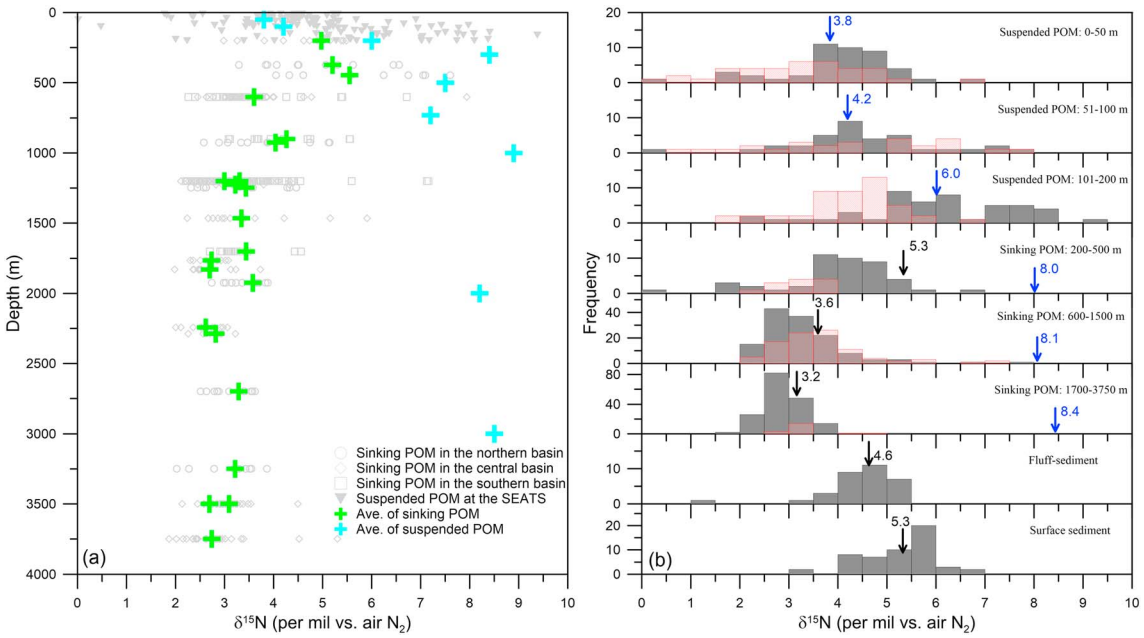

Figure 7. (a) Vertical distributions of the $\delta^{15}N$ values in suspended ($\delta^{15}N_{sus}$) and sinking POM ($\delta^{15}N_{sink}$) and their averages in the SCS. (b) Histograms of the $\delta^{15}N_{sus}$ and $\delta^{15}N_{sink}$ values at different depth intervals in the northern and central (gray) and southern (red diagonal) basins and the $\delta^{15}N$ values (gray) in the fluff and surface sediments for the entire basin are presented. The blue arrows in Figure 7b indicate the average $\delta^{15}N_{sus}$ values, and the black arrows indicate the average $\delta^{15}N$ values in sinking POM and the fluff and surface sediments, respectively. Data source is shown in Table 1. The northern basin includes the M1S and M2S sites; the central basin contains the SEATS, SCS-NE, SCS-NC, and SCS-C sites, and the southern basin corresponds to the SCS-SW, SCS-SC and SCS-S sites (see text).

Finally, the decreasing trend in $\delta^{15}N_{sink}$ could possibly be attributable to the preferential export of small phytoplankton to the deep ocean. *Puigcorbé et al.* [2015] reported that picoplankton—rather than diatom—dominated food webs have the highest export efficiencies and can be a major contributor to the sinking particle in the subtropical regions. The $\delta^{15}N$ values in *Prochlorococcus* were found to be much lower than those in eukaryotes (larger sizes) in the Sargasso Sea [*Fawcett et al.*, 2011]. In the summer SCS picoplankton occupy up to ~80% of the total autotrophic biomass in surface waters [*Wong et al.*, 2007], raising the possibility of preferential export of small phytoplankton. In fact, the latest genomic study revealed that substantial amounts of *Prochlorococcus* populations can be found in the deep waters of the SCS and LS [*Jiao et al.*, 2014], which is supportive of the hypothesis of $\delta^{15}N_{sink}$ shift by small phytoplankton although the mechanism is not well understood. Flow cytometry-IRMS technique is not yet applied in the SCS to discern isotopic compositions of *Prochlorococcus* and picoeukaryotes. Further studies are urgently needed to assess N isotopic signals of small prokaryotes and its contribution to deep PNF in the SCS in terms of N isotope perspective, which will be helpful to understand the transfer processes of the PN isotope signal in the deep basin.

4.3. Sinking Versus Suspended Particulate N Isotopic Alteration

Based on the compilation of all $\delta^{15}N$ data in particulate and sedimentary N (Figure 7), we examine the $\delta^{15}N$ alteration of POM from production to deposition into the sediments in the SCS basin. As mentioned above, the observed $\delta^{15}N_{sink}$ values (4.4‰) exported from the EZ well reflect the $\delta^{15}N$ of subsurface nitrate. Around 1‰ increase for the $\delta^{15}N_{sink}$ collected at ~500 m (average of ~5.3‰; Figures 4 and 7a) suggests that remineralization may have occurred. Below ~500 m, $\delta^{15}N_{sink}$ presents a downward decreasing trend (3.2‰ at 3000–4000 m), which is attributable to the influences of lateral transport with additional incorporation of light-N by bacteria, and/or preferential export of small phytoplankton. As aforementioned, such a decreasing pattern in $\delta^{15}N_{sink}$ has been reported in regions of low export fluxes [e.g., *Altabet et al.*, 1991; *Nakatsuka et al.*, 1997] and in anaerobic water [e.g., *Lehmann et al.*, 2002]. In marginal regions and most open oceans, the $\delta^{15}N_{sink}$ alteration in the water column is thought to be minimal in the water column [*Robinson et al.*, 2012]. Our results show that, in fact, a similar pattern of the declining $\delta^{15}N_{sink}$ has occurred in the marginal sea featured by moderate production and oxic conditions.

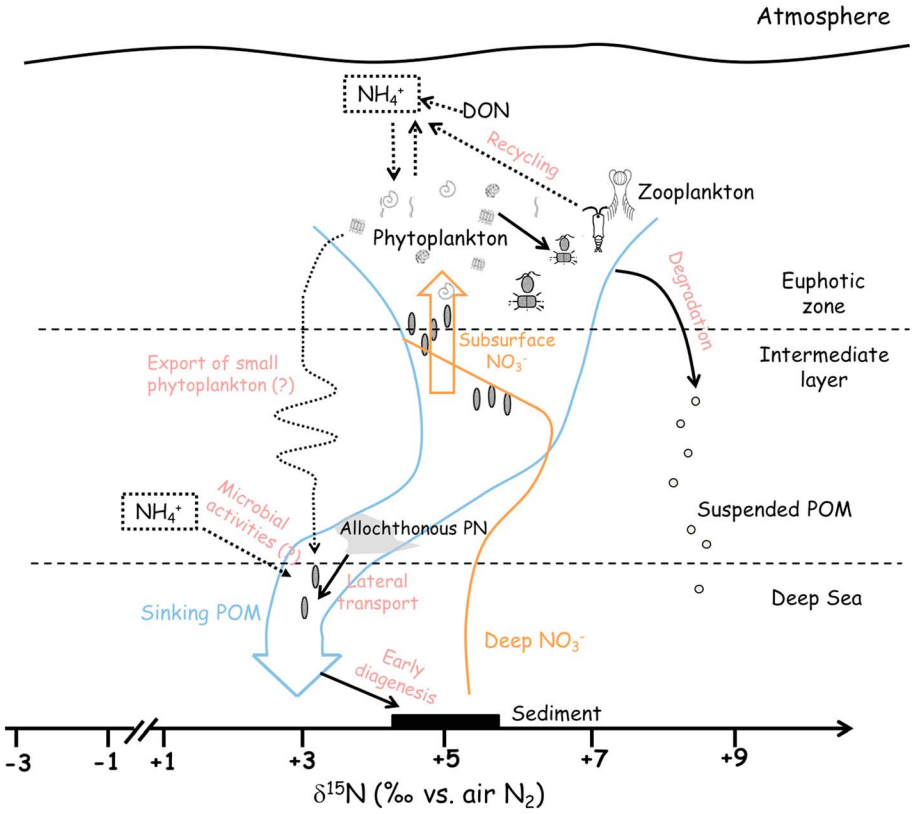

Figure 8. Conceptual diagram of the $\delta^{15}N$ values of different N species and N processes that determine their distribution in the SCS. The orange curve and light blue arrow show the $\delta^{15}N_{NO3}$ distribution and the $\delta^{15}N$ trend of sinking POM in the northern SCS, respectively. The symbols for dissolved and other particulate phases correspond to their average $\delta^{15}N$ values on the axis.

In Figure 7b, we find a statistically positive shift (~2‰, $p < 0.05$) in surface sedimentary $\delta^{15}N$ values ($\delta^{15}N_{sed}$, with an average of 5.3 ± 0.7‰) relative to the $\delta^{15}N_{sink}$ values in the deep waters. Such positive $\delta^{15}N$ shift has been attributable to degradation of organic matter via early diagenetic reactions [*Gaye et al.*, 2009] and the degree of shift is positively correlated with the oxygen exposure time [*Robinson et al.*, 2012]. Obviously, the diagenetic induced positive shift of $\delta^{15}N$ is compensated by negative shifts in the water column. The shifted $\delta^{15}N_{sed}$ values are identical to the $\delta^{15}N$ values of subsurface nitrate and shallow sinking POM due to remarkable $\delta^{15}N$ alterations occurred during sinking and postdeposition. Whether the $\delta^{15}N_{sed}$ truthfully archived the subsurface nitrate is thus doubtful. Moreover, clay mineral evidence illustrates that the relative contributions of lithogenic particles from the adjacent land present a distinct variability from the last glaciation to the Holocene [e.g., *Liu et al.*, 2016]. Since the clay-fixed N may carry the climate information from land and the occupation of clay-fixed N in total N is relatively high in China's marginal seas [*Zheng et al.*, 2015], it is conceivable that changes in climate and the sediment source region may have also led to the variability of downcore $\delta^{15}N_{sed}$.

On the other hand, suspended and sinking particles contain very different $\delta^{15}N$ values (Figure 7). The vertical pattern of $\delta^{15}N_{sus}$ is inconsistent to the downward decreasing trend of $\delta^{15}N_{sink}$ in the SCS basin. The $\delta^{15}N_{sus}$ values increase dramatically downward from ~4‰ in the EZ to 8‰ at ~500 m and remain constant (8.2 ± 0.2‰) below 500 m (Figure 7). The increase in $\delta^{15}N_{sus}$ below the EZ has been primarily interpreted as preferential degradation of light N in fresh POM [e.g., *Altabet*, 1988]. However, unchanged yet distinctively high $\delta^{15}N_{sus}$ values in the mesopelagic zone may not be as a result of preferential decomposition of light N as that in the upper water column. The suspended POM in the deep ocean may partly originate from disaggregation and solubilization of sinking POM by attached bacteria [e.g., *Collins et al.*, 2015]. If these processes prevail, we should not see distinctive $\delta^{15}N$ values between suspended and sinking particles. In fact, the significant deviation between $\delta^{15}N_{sus}$ and $\delta^{15}N_{sink}$ may not support the above processes determining

deep $\delta^{15}N_{sus}$. Meanwhile, the AA composition of suspended POM in the subthermocline water column was found to be different from those in sinking POM and mixed-layer suspended matter [*Gaye et al*., 2013]. By using a shotgun proteomic approach, a recent study in the SCS basin further indicated that the sources of midwater suspended POM depart from those of surface POM [*Dong et al*., 2010]. Unfortunately, few isotope surveys have been carried out for specific N compounds regarding suspended and sinking particles. Moreover, *Gaye et al*. [2013] speculated that the uniform $\delta^{15}N_{sus}$ in the deep ocean may be due to the long residence time of fine particles and their exchange with the homogenous dissolved organic matter (DOM). Analogous to the hypothesis of disaggregation of sinking POM, isotopic fractionation is required during the exchange with DOM unless the DOM in the deep waters contains $\delta^{15}N$ values as high as those of $\delta^{15}N_{sus}$. Again, no isotopic data for the DON are reported for the deep ocean (>300 m) due to technical difficulties [*Knapp et al*., 2011]. Different approaches, such as proteomics and compound specific isotope analyses, are needed to explore the causes for the significant deviation between $\delta^{15}N_{sus}$ and $\delta^{15}N_{sink}$ and the mechanisms to maintain uniform $\delta^{15}N_{sus}$ values in the deep ocean.

5. Conclusions and Implications

With attempt to unravel N transformation in the EZ and N isotopic alteration of POM from surface production to burial in the deep ocean (Figure 8), for the first time we examine N isotopes in the dissolved and particulate pools in the SCS basin by a compilation of new and published data sets. Subsurface $\delta^{15}N_{NO3}$ in the northern SCS shows a spatially homogeneous pattern, which is significantly different from that in the WPS. The $\delta^{15}N_{NO3}$ values in the SCS subsurface are close to $\delta^{15}N_{sink}$ from the EZ, suggesting that subsurface nitrate plays a major role in supporting export production and the isotopic signature of sinking POM at initial stage. Similar $\delta^{15}N$ values (mostly spanning 4–6‰) are found among suspended/sinking POM, zooplankton in the EZ, and subsurface nitrate, thus implying that new and recycled N may possess comparable N isotopic compositions unless the reported *f* ratios are incorrect. Alternatively, remineralization supported by DON ($\delta^{15}N$ value of 5‰) input from lateral exchange with the WPS and/or rapid N turnover among the different N species is suggested to maintain the isotopic compositions among pools within a narrow range, which is unusual when compared with other oligotrophic oceans.

Allochthonous PN addition caused by lateral advection from a nearby canyon off Taiwan contributes to the elevated PNF in the deep waters. The canyon sediments account for more than 50% of the PNF in the deep waters especially in the northern SCS basin. Canyon introduces ^{15}N-depleted signals to bias the normally unchanged $\delta^{15}N_{sink}$ toward lower values. Besides the lateral input, the further drawdown of $\delta^{15}N_{sink}$ during downward transit of sinking particles in the deep waters might be caused by the incorporation of lighter N from bacteria and/or preferential export of small phytoplankton. However, we cannot exclude the contribution from terrigenous organics in surface soil or vegetation due to limited information for this specific endmember. The mechanisms to maintain constant yet distinctively high $\delta^{15}N$ in the suspended particles relative to those in sinking POM in the deep waters remain unknown. However, it contradicts the hypothesis of a rapid exchange between suspended and sinking particles.

Since the down-core $\delta^{15}N_{sed}$ records are often used to reconstruct past changes in local N sources, N cycling processes, and the oceanic N inventory [*Higginson et al*., 2003; *Kienast*, 2000], our findings highlight the multiple processes and different origins of particles that have led to remarkable $\delta^{15}N$ alterations of POM throughout the water column and in the surface sediments within the SCS. The fidelity of bulk $\delta^{15}N_{sed}$ has been determined in many marginal seas and continental regions, where $\delta^{15}N$ alteration is minor. However, our results suggest that even in marginal seas intensive $\delta^{15}N$ alteration in the water column should be carefully evaluated prior to using bulk $\delta^{15}N_{sed}$ as a modern and paleo indicator.

Acknowledgments
Group members of Kao's laboratory in Academia Sinica (Taiwan) and the Ocean Carbon Group led by Dai in Xiamen University are gratefully acknowledged for their assistance in sample analysis. We also thank the crew members of the R/V *Dongfanghong II*. We wish to gratefully acknowledge the valuable comments and suggestions of this manuscript by all anonymous reviewers and also the support of the JGR-Biogeosciences Editor Miguel Goni. Finally, we thank John Hodgkiss for his help with English. This work was funded by the National Basic Research Program (973) sponsored by the Ministry of Science and Technology, China (grants 2014CB953702 and 2015CB954003), and the National Natural Science Foundation of China through grants 41130857, 91328207, 91328202, 91428308, and 41176059. The data used are available at https://doi.pangaea.de/10.1594/PANGAEA.876444.

References

Altabet, M. A. (1988), Variations in nitrogen isotopic composition between sinking and suspended particles: Implications for nitrogen cycling and particle transformation in the open ocean, *Deep Sea Res., Part A*, *35*(4), 535–554, doi:10.1016/0198-0149(88)90130-6.

Altabet, M. A. (2001), Nitrogen isotopic evidence for micronutrient control of fractional NO_3^- utilization in the equatorial Pacific, *Limnol. Oceanogr.*, *46*(2), 368–380, doi:10.4319/lo.2001.46.2.0368.

Altabet, M. A., and R. Francois (1994), Sedimentary nitrogen isotopic ratio as a recorder for surface ocean nitrate utilization, *Global Biogeochem. Cycles*, *8*, 103–116, doi:10.1029/93GB03396.

Altabet, M. A., W. G. Deuser, S. Honjo, and C. Stienen (1991), Seasonal and depth-related changes in the source of sinking particles in the North Atlantic, *Nature*, *354*(6349), 136–139, doi:10.1038/354136a0.

Bourbonnais, A., M. F. Lehmann, J. J. Waniek, and D. E. Schultz-Bull (2009), Nitrate isotope anomalies as indicator of N_2 fixation in the Azores Front region (subtropical NE Atlantic), *J. Geophys. Res.*, *114*, C03003, doi:10.1029/2007JC004617.

Cai, P. H., D. C. Zhao, L. Wang, B. Q. Huang, and M. H. Dai (2015), Role of particle stock and phytoplankton community structure in regulating particulate organic carbon export in a large marginal sea, *J. Geophys. Res. Oceans*, *120*, 2063–2095, doi:10.1002/2014JC010432.

Casciotti, K. L., T. W. Trull, D. M. Glover, and D. Davies (2008), Constraints on nitrogen cycling at the subtropical North Pacific Station ALOHA from isotopic measurements of nitrate and particulate nitrogen, *Deep Sea Res., Part II*, *55*(14–15), 1661–1672, doi:10.1016/j.dsr2.2008.04.017.

Chen, Y. L. L. (2005), Spatial and seasonal variations of nitrate-based new production and primary production in the South China Sea, *Deep Sea Res., Part I*, *52*, 319–340, doi:10.1016/j.dsr.2004.11.001.

Chen, Y. L. L., H. Y. Chen, S. H. Tuo, and K. Ohki (2008), Seasonal dynamics of new production from *Trichodesmium* N_2 fixation and nitrate uptake in the upstream Kuroshio and South China Sea basin, *Limnol. Oceanogr.*, *53*(5), 1705–1721, doi:10.4319/lo.2008.53.5.1705.

Chung, Y., H. C. Chang, and G. W. Hung (2004), Particulate flux and ^{210}Pb determined on the sediment trap and core samples from the northern South China Sea, *Cont. Shelf Res.*, *24*(6), 673–691, doi:10.1016/j.csr.2004.01.003.

Collins, J. R., B. R. Edwards, K. Thamatrakoln, J. E. Ossolinski, G. R. DiTullio, K. D. Bidle, S. C. Doney, and B. A. S. Van Mooy (2015), The multiple fates of sinking particles in the North Atlantic Ocean, *Global Biogeochem. Cycles*, *29*, 1471–1494, doi:10.1002/2014GB005037.

Dai, M., Z. Cao, X. Guo, W. Zhai, Z. Liu, Z. Yin, Y. Xu, J. Gan, J. Hu, and C. Du (2013), Why are some marginal seas sources of atmospheric CO_2?, *Geophys. Res. Lett.*, *40*, 2154–2158, doi:10.1002/grl.50390.

Dong, H. P., D. Z. Wang, M. Dai, and H. S. Hong (2010), Characterization of particulate organic matter in the water column of the South China Sea using a shotgun proteomic approach, *Limnol. Oceanogr.*, *55*(4), 1565–1578, doi:10.4319/lo.2010.55.4.1565.

Du, C., Z. Liu, M. Dai, S. J. Kao, Z. Cao, Y. Zhang, T. Huang, L. Wang, and Y. Li (2013), Impact of the Kuroshio intrusion on the nutrient inventory in the upper northern South China Sea: Insights from an isopycnal mixing model, *Biogeosciences*, *10*, 6419–6432, doi:10.5194/bg-10-6419-2013.

Fawcett, S. E., M. W. Lomas, J. R. Casey, B. B. Ward, and D. M. Sigman (2011), Assimilation of upwelled nitrate by small eukaryotes in the Sargasso Sea, *Nat. Geosci.*, *4*, 717–722, doi:10.1038/NGEO1265.

Freudenthal, T., S. Neuer, H. Meggers, R. Davenport, and G. Wefer (2001), Influence of lateral particle advection and organic matter degradation on sediment accumulation and stable nitrogen isotope ratios along a productivity gradient in the Canary Islands region, *Mar. Geol.*, *177*, 93–109, doi:10.1016/S0025-3227(01)00126-8.

Gaye, B., M. G. Wiesner, and N. Lahajnar (2009), Nitrogen sources in the South China Sea, as discerned from stable nitrogen isotopic ratios in rivers, sinking particles, and sediments, *Mar. Chem.*, *114*(3–4), 72–85, doi:10.1016/j.marchem.2009.04.003.

Gaye, B., B. Nagel, K. Dähnke, T. Rixen, N. Lahajnar, and K. C. Emeis (2013), Amino acid composition and δ^{15}N of suspended matter in the Arabian Sea: Implications for organic matter sources and degradation, *Biogeosciences*, *10*(11), 7689–7702, doi:10.5194/bg-10-7689-2013.

Granger, J., and D. M. Sigman (2009), Removal of nitrite with sulfamic acid for nitrate N and O isotope analysis with the denitrifier method, *Rapid Commun. Mass Spectrom.*, *23*(23), 3753–3762, doi:10.1002/rcm.4307.

Hannides, C. C. S., B. N. Popp, C. A. Choy, and J. C. Drazen (2013), Midwater zooplankton and suspended particle dynamics in the North Pacific Subtropical Gyre: A stable isotope perspective, *Limnol. Oceanogr.*, *58*(6), 1931–1946, doi:10.4319/lo.2013.58.6.1931.

Higginson, M. J., J. R. Maxwell, and M. A. Altabet (2003), Nitrogen isotope and chlorin paleoproductivity records from the Northern South China Sea: Remote vs. local forcing of millennial- and orbital-scale variability, *Mar. Geol.*, *201*(1–3), 223–250, doi:10.1016/S0025-3227(03)00218-4.

Hu, J. F., P. A. Peng, G. D. Jia, B. X. Mai, and G. Zhang (2006), Distribution and sources of organic carbon, nitrogen and their isotopes in sediments of the subtropical Pearl River estuary and adjacent shelf, Southern China, *Mar. Chem.*, *98*(2–4), 274–285, doi:10.1016/j.marchem.2005.03.008.

Huh, C. A., J. T. Liu, H. L. Lin, and J. P. Xu (2009), Tidal and flood signatures of settling particles in the Gaoping submarine canyon (SW Taiwan) revealed from radionuclide and flow measurements, *Mar. Geol.*, *267*, 8–17, doi:10.1016/j.margeo.2009.09.001.

Jiao, N., et al. (2014), Presence of *Prochlorococcus* in the aphotic waters of the western Pacific Ocean, *Biogeosciences*, *11*(8), 2391–2400, doi:10.5194/bg-11-2391-2014.

Kao, S. J., and K. K. Liu (2000), Stable carbon and nitrogen isotope systematics in a human-disturbed watershed (Lanyang-Hsi) in Taiwan and the estimation of biogenic particulate organic carbon and nitrogen fluxes, *Global Biogeochem. Cycles*, *14*(1), 189–198, doi:10.1029/1999GB900079.

Kao, S. J., F. K. Shiah, C. H. Wang, and K. K. Liu (2006), Efficient trapping of organic carbon in sediments on the continental margin with high fluvial sediment input off southwestern Taiwan, *Cont. Shelf Res.*, *26*, 2520–2537, doi:10.1016/j.csr.2006.07.030.

Kao, S. J., M. H. Dai, K. Y. Wei, N. E. Blair, and W. B. Lyons (2008), Enhanced supply of fossil organic carbon to the Okinawa trough since the last deglaciation, *Paleoceanography*, *23*, PA2207, doi:10.1029/2007PA001440.

Kao, S. J., M. Dai, K. Selvaraj, W. Zhai, P. Cai, S. N. Chen, J. Y. T. Yang, J. T. Liu, C. C. Liu, and J. P. M. Syvitski (2010), Cyclone-driven deep sea injection of freshwater and heat by hyperpycnal flow in the subtropics, *Geophys. Res. Lett.*, *37*, L21702, doi:10.1029/2010GL044893.

Kao, S. J., J. Y. T. Yang, K. K. Liu, M. H. Dai, W. C. Chou, H. L. Lin, and H. J. Ren (2012), Isotope constraints on particulate nitrogen source and dynamics in the upper water column of the oligotrophic South China Sea, *Global Biogeochem. Cycles*, *26*, GB2033, doi:10.1029/2011GB004091.

Kao, S. J., B. Y. Wang, L. W. Zheng, K. Selvaraj, S. C. Hsu, X. H. S. Wan, M. Xu, and C. T. A. Chen (2015), Spatiotemporal variations of nitrogen isotopic records in the Arabian Sea, *Biogeosciences*, *12*, 1–14, doi:10.5194/bg-12-1-2015.

Kienast, M. (2000), Unchanged nitrogen isotopic composition of organic matter in the South China Sea during the last climatic cycle: Global implications, *Paleoceanography*, *15*(2), 244–253, doi:10.1029/1999PA000407.

Kienast, M., M. J. Higginson, G. Mollenhauer, T. I. Eglinton, M. T. Chen, and S. E. Calvert (2005), On the sedimentological origin of down-core variations of bulk sedimentary nitrogen isotope ratios, *Paleoceanography*, *20*, PA2009, doi:10.1029/2004PA001081.

Knapp, A. N., D. M. Sigman, F. Lipschultz, A. B. Kustka, and D. G. Capone (2011), Interbasin isotopic correspondence between upper-ocean bulk DON and subsurface nitrate and its implications for marine nitrogen cycling, *Global Biogeochem. Cycles*, *25*, GB4004, doi:10.1029/2010GB003878.

Koppelmann, R., R. Böttger-Schnack, J. Möbius, and H. Weikert (2009), Trophic relationships of zooplankton in the eastern Mediterranean based on stable isotope measurements, *J. Plankton Res.*, *31*(6), 669–686, doi:10.1093/plankt/fbp013.

Lahajnar, N., M. G. Wiesner, and B. Gaye (2007), Fluxes of amino acids and hexosamines to the deep South China Sea, *Deep Sea Res., Part I*, *54*(12), 2120–2144, doi:10.1016/j.dsr.2007.08.009.

Lehmann, M. F., S. M. Bernasconi, A. Barbieri, and J. A. McKenzie (2002), Preservation of organic matter and alteration of its carbon and nitrogen isotope composition during simulated and in situ early sedimentary diagenesis, *Geochim. Cosmochim. Acta*, *66*(20), 3573–3584, doi:10.1016/S0016-7037(02)00968-7.

Letscher, R. T., D. A. Hansell, C. A. Carlson, R. Lumpkin, and A. N. Knapp (2013), Dissolved organic nitrogen in the global surface ocean: Distribution and fate, *Global Biogeochem. Cycles*, *27*, 141–153, doi:10.1029/2012GB004449.

Liang, Y. J. (2008), Depth and temporal variability of organic carbon, total nitrogen and their isotopic compositions of sinking particulate organic matter and POC flux at SEATS time-series station, northern South China Sea [in Chinese with an English abstract], M.S. thesis, National Sun Yat-sen University, Kaohsing, Taiwan.

Liu, K. K., M. J. Su, C.-R. Hsueh, and G. C. Gong (1996), The nitrogen isotopic composition of nitrate in the Kuroshio Water northeast of Taiwan: Evidence for nitrogen fixation as a source of isotopically light nitrate, *Mar. Chem.*, *54*(3–4), 273–292, doi:10.1016/0304-4203(96)00034-5.

Liu, K. K., S. Y. Chao, P. T. Shaw, G. C. Gong, C. C. Chen, and T. Y. Tang (2002), Monsoon-forced chlorophyll distribution and primary production in the South China Sea: Observations and a numerical study, *Deep Sea Res., Part I*, *49*(8), 1387–1412, doi:10.1016/S0967-0637(02)00035-3.

Liu, K. K., S. J. Kao, H. C. Hu, W. C. Chou, G. W. Hung, and C. M. Tseng (2007), Carbon isotopic composition of suspended and sinking particulate organic matter in the northern South China Sea—From production to deposition, *Deep Sea Res., Part II*, *54*(14–15), 1504–1527, doi:10.1016/j.dsr2.2007.05.010.

Liu, K. K., C. M. Tseng, C. R. Wu, and I. I. Lin (2010), The South China Sea, in *Carbon and Nutrient Fluxes in Continental Margins: A Global Synthesis*, edited by K. K. Liu et al., pp. 124–146, Springer, Berlin, doi:10.1007/978-3-540-92735-8.

Liu, Z. F., et al. (2010), Clay mineral distribution in surface sediments of the northeastern South China Sea and surrounding fluvial drainage basins: Source and transport, *Mar. Geol.*, *277*, 48–60, doi:10.1016/j.margeo.2010.08.010.

Liu, Z. F., et al. (2016), Source-to-sink transport processes of fluvial sediments in the South China Sea, *Earth Sci. Rev.*, *153*, 238–273, doi:10.1016/j.earscirev.2015.08.005.

Loick, N., J. Dippner, H. N. Doan, I. Liskow, and M. Voss (2007), Pelagic nitrogen dynamics in the Vietnamese upwelling area according to stable nitrogen and carbon isotope data, *Deep Sea Res., Part I*, *54*(4), 596–607, doi:10.1016/j.dsr.2006.12.009.

Mahaffey, C., C. R. Benitez-Nelson, R. R. Bidigare, Y. Rii, and D. M. Karl (2008), Nitrogen dynamics within a wind-driven eddy, *Deep Sea Res., Part II*, *55*(10–13), 1398–1411, doi:10.1016/j.dsr.2008.02.004.

Martin, J. H., G. A. Knauer, D. M. Karl, and W. W. Broenkow (1987), VERTEX: Carbon cycling in the northeast Pacific, *Deep Sea Res., Part A*, *34*, 267–285, doi:10.1016/0198-0149(87)90086-0.

McCarthy, M. D., R. Benner, C. Lee, and M. L. Fogel (2007), Amino acid nitrogen isotopic fractionation patterns as indicators of heterotrophy in plankton, particulate, and dissolved organic matter, *Geochim. Cosmochim. Acta*, *71*, 4727–4744, doi:10.1016/j.gca.2007.06.061.

Mino, Y., T. Saino, K. Suzuki, and E. Maranon (2002), Isotopic composition of suspended particulate nitrogen ($\delta^{15}N_{sus}$) in surface waters of the Atlantic Ocean from 50°N to 50°S, *Global Biogeochem. Cycles*, *16*(4), 1059, doi:10.1029/2001GB001635.

Montoya, J. P., E. J. Carpenter, and D. G. Capone (2002), Nitrogen fixation and nitrogen isotope abundances in zooplankton of the oligotrophic North Atlantic, *Limnol. Oceanogr.*, *47*(6), 1617–1628, doi:10.4319/lo.2002.47.6.1617.

Nakatsuka, T., N. Handa, N. Harada, T. Sugimoto, and S. Imaizumi (1997), Origin and decomposition of sinking particulate organic matter in the deep water column inferred from the vertical distributions of its $\delta^{15}N$, $\delta^{13}C$ and $\delta^{14}C$, *Deep Sea Res., Part I*, *44*(12), 1957–1979, doi:10.1016/S0967-0637(97)00051-4.

Puigcorbé, V., C. R. Benitez-Nelson, P. Masqué, E. Verdeny, A. E. White, B. N. Popp, F. G. Prahl, and P. J. Lam (2015), Small phytoplankton drive high summertime carbon and nutrient export in the Gulf of California and Eastern Tropical North Pacific, *Global Biogeochem. Cycles*, *29*, 1309–1332, doi:10.1002/2015GB005134.

Rafter, P. A., D. M. Sigman, C. D. Charles, J. Kaiser, and G. H. Haug (2012), Subsurface tropical Pacific nitrogen isotopic composition of nitrate: Biogeochemical signals and their transport, *Global Biogeochem. Cycles*, *26*, GB1003, doi:10.1029/2010GB003979.

Ren, H., Y.-C. Chen, X. T. Wang, G. T. F. Wong, A. L. Cohen, T. M. DeCarlo, M. A. Weigand, H.-S. Mii, and D. M. Sigman (2017), 21st-century rise in anthropogenic nitrogen deposition on a remote coral reef, *Science*, *356*(6339), 749–752, doi:10.1126/science.aal3869.

Robinson, R. S., et al. (2012), A review of nitrogen isotopic alteration in marine sediments, *Paleoceanography*, *27*, PA4203, doi:10.1029/2012PA002321.

Saino, T., and A. Hattori (1987), Geographical variation of the water column distribution of suspended particulate organic nitrogen and its ^{15}N natural abundance in the Pacific and its marginal seas, *Deep Sea Res., Part A*, *34*(5–6), 807–827, doi:10.1016/0198-0149(87)90038-0.

Schroeder, A., M. G. Wiesner, and Z. Liu (2015), Fluxes of clay minerals in the South China Sea, *Earth Planet. Sci. Lett.*, *430*, 30–42, doi:10.1016/j.epsl.2015.08.001.

Selvaraj, K., T. Y. Lee, J. Y. T. Yang, E. A. Canuel, J. C. Huang, M. H. Dai, and S. J. Kao (2015), Stable isotopic and biomarker evidence of terrigenous organic matter export to the deep sea during tropical storms, *Mar. Geol.*, *364*, 32–42, doi:10.1016/j.margeo.2015.03.005.

Sigman, D. M., M. A. Altabet, D. C. McCorkle, R. Francois, and G. Fischer (2000), The $\delta^{15}N$ of nitrate in the Southern Ocean: Nitrogen cycling and circulation in the ocean interior, *J. Geophys. Res.*, *105*(C8), 19599–19614, doi:10.1029/2000JC000265.

Sigman, D. M., K. L. Casciotti, M. Andreani, C. Barford, M. Galanter, and J. K. Bohlke (2001), A bacterial method for the nitrogen isotopic analysis of nitrate in seawater and freshwater, *Anal. Chem.*, *73*(17), 4145–4153, doi:10.1021/ac010088e.

Sigman, D. M., P. J. DiFiore, M. P. Hain, C. Deutsch, and D. M. Karl (2009), Sinking organic matter spreads the nitrogen isotope signal of pelagic denitrification in the North Pacific, *Geophys. Res. Lett.*, *36*, L08605, doi:10.1029/2008GL035784.

Shiozaki, T., K. Furuya, T. Kodama, S. Kitajima, S. Takeda, T. Takemura, and J. Kanda (2010), New estimation of N_2 fixation in the western and central Pacific Ocean and its marginal seas, *Global Biogeochem. Cycles*, *24*, GB1015, doi:10.1029/2009GB003620.

Wong, G. T. F., S. W. Chung, F. K. Shiah, C. C. Chen, L. S. Wen, and K. K. Liu (2002), Nitrate anomaly in the upper nutricline in the northern South China Sea—Evidence for nitrogen fixation, *Geophys. Res. Lett.*, *29*(23), 2097, doi:10.1029/2002GL015796.

Wong, G. T. F., T. L. Ku, M. Mulholland, C. M. Tseng, and D. P. Wang (2007), The SouthEast Asian time-series study (SEATS) and the biogeochemistry of the South China Sea—An overview, *Deep Sea Res., Part II*, *54*(14–15), 1434–1447, doi:10.1016/j.dsr2.2007.05.012.

Wu, K., M. Dai, J. Chen, F. Meng, X. Li, Z. Liu, C. Du, and J. Gan (2015), Dissolved organic carbon in the South China Sea and its exchange with the Western Pacific Ocean, *Deep Sea Res., Part II*, *122*, 41–51, doi:10.1016/j.dsr2.2015.06.013.

Yang, J. Y. T., S. C. Hsu, M. H. Dai, S. S. Y. Hsiao, and S. J. Kao (2014), Isotopic composition of water-soluble nitrate in bulk atmospheric deposition at Dongsha Island: Sources and implications of external N supply to the northern South China Sea, *Biogeosciences*, *11*, 1833–1846, doi:10.5194/bg-11-1833-2014.

Yang, J. Y. T., S. J. Kao, M. H. Dai, X. Yan, and H. L. Lin (2017), N isotopic signals in nitrate and particulate phases, datasets for figures and table, *PANGEA*, doi:10.1594/PANGAEA.876444.

You, Y., C. S. Chern, Y. Yang, C. T. Liu, K. K. Liu, and S. C. Pai (2005), The South China Sea, a *cul-de-sac* of North Pacific Intermediate Water, *J. Oceanogr.*, *61*, 509–527, doi:10.1007/s10872-005-0059-6.

Zhang, Y., K. Kaiser, L. Li, D. Zhang, Y. Ran, and R. Benner (2014), Sources, distributions, and early diagenesis of sedimentary organic matter in the Pearl River region of the South China Sea, *Mar. Chem.*, *158*, 39–48, doi:10.1016/j.marchem.2013.11.003.

Zheng, L. W., S. S. Y. Hsiao, X. D. Ding, D. Li, Y. P. Chang, and S. J. Kao (2015), Isotopic composition and speciation of sedimentary nitrogen and carbon in the Okinawa Trough over the past 30 ka, *Paleoceanography*, *30*, 1233–1244, doi:10.1002/2015PA002782.